doi: 10.6062/jcis.2016.07.03.0113 Discussion Paper Cunha & Homem

A hybrid approach based on Projections Onto Convex Sets for Spatial and Spectral Super-Resolution

Bruno Aguilar da Cunha[a1], Murillo Rodrigo Petrucelli Homem [a]

[a]Federal University of São Carlos (UFSCar), Brazil

Received on December 04, 2016 / accepted on December 30, 2016

Abstract

This work proposes both a study and a development of an algorithm for super-resolution of digital images using projections onto convex sets. The method is based on a classic algorithm for spatial super-resolution which considering the subpixel information present in a set of lower resolution images, generate an image of higher resolution and better visual quality. We propose the incorporation of a new restriction based on the Richardson-Lucy algorithm in order to restore and recover part of the spatial frequencies lost during the degradation and decimation process of the high resolution images. In this way the algorithm provides a hybrid approach based on projections onto convex sets which is capable of promoting both the spatial and spectral image super-resolution. The proposed approach was compared with the original algorithm from Sezan and Tekalp and later with a method based on a robust framework that is considered nowadays one of the most effective methods for super-resolution. The results, considering both the visual and the mean square error analysis, demonstrate that the proposed method has great potential promoting increased visual quality over the images studied.

Keywords: Super-Resolution, POCS, Spectral Approach, Hybrid Approach.

1. Introduction

The term spatial resolution in image processing can be defined as the smallest perceivable or discernable detail in a digital image and is strictly related to the visual quality and the fidelity of what is represented in relation to a real scene [1, 2]. The larger the spatial resolution of an image, the greater the number of pixels in a given area and the smaller the dimensions of a single

[1]E-mail Corresponding Author: brunoaguilar@msn.com

pixel to be represented, allowing for better definition of the details and a smoother transition between the colors [2].

Super Resolution (SR) [3] is a well-known signal processing technique, which aims at obtaining a high resolution image (HR) through one or more low resolution images of the same scene. The term "super" alludes to the ability of the art to overcome the inherent limitations of low resolution (LR) imaging systems. A great differential of the technique, is the possibility of obtaining the images with better spatial resolution, from images of these already existing systems, without the need for improvements in the acquisition process. Therefore, the Super-Resolution aims to increase the image size (also increasing the number of pixels and the resolution of the image) and reduce the inherent degradations of the LR images used. [4].

We present a methodology to obtain a high resolution estimate considering low resolution images through Projection Onto Convex Sets (POCS) considering a hybrid approach in which super-resolution occurs in the context in addition to increasing the size of the high-resolution image, it also seeks to recover high lost frequencies while at the same time decreasing blurring and degradation in order to approximate or overcome a chosen technique in which the results are quite appreciable, using a Robust Super-Resolution framework [5, 6]. Another important issue is the possibility of aggregating classical methods in the POCS approach with other approaches in the literature through convex sets that can provide results that meet the desired needs.

2. Image Super-Resolution

Super-resolution reconstruction of images can be seen as a three-stage process [7]. The first step is to register in order to align the low resolution images with subpixel precision in relation to a reference image that usually corresponds to one of the available low resolution images. Next, the next step is to construct a higher resolution grid from the aligned images, and finally, the high resolution image restoration is conducted to remove the blurring from the acquisition process. The figure 1, illustrates the first two phases of this process. Considering that the image of the upper left corner is the reference image, the other two are aligned with respect to it, and in sequence a higher resolution grid is generated from the alignment.

If the displacements are non-integers, however they have the same values for all images, the interpolation will be on a uniform grid [3, 8, 9]. On the other hand, in the more general case, when the images have arbitrary displacements, non-uniform interpolation is required. This procedure is one

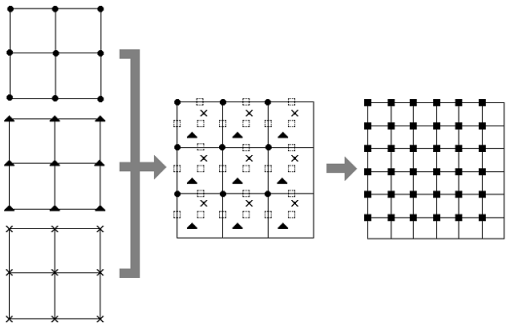

Figure 1: Interpolation from a non-uniform grid

of the most intuitive mechanisms for achieving super-resolution. The problem of super-resolution is defined as a ill conditioned process, that is, in the sense that the solution may not exist, or it may not be unique, or it may not depend on the data in a continuous way [9].

2.1 Image observation model

The digital imaging system is imperfect and due to hardware limitations, during the acquisition process, several types of degradations occur [4]. An example is optical blurring, caused by the finite aperture during capture of the scene by the equipment. This type of blurring, also present in videos, is modeled and represented by the Point Spread Function (PSF).

Consider $f[i,j]$, $0 \leq i,j \leq M$, an ideal image without degradation and conveniently sampled according to the Nyquist limit, from a scene of interest $f : \Re^2 \rightarrow \Re$.In a realistic situation, the digital image is usually blurred by the acquisition system and also corrupted by some kind of noise.

In this sense, from a pixel ordering, a degraded and low-resolution version $g_k[k,l]$, $0 \leq k,l \leq N$, $N \leq M$, from a high resolution image f, can be modeled by [10]

$$g_k = H_k D_k f + n_k, \tag{1}$$

where n_k represents the noise in the observation g_k, following an additive model.

For the blurring operator, a matrix of $N^2 \times N^2$ dimension is often considered. In other words, we use a spatially invariant linear operator, where the elements are samples of the point spread function (PSF) that represents the degradation mechanism [7].

We observe that, according to the position of the acquisition sensors, the decimation operator $D_k[u,v]$ and $0 \leq v \leq M^2$, may be responsible for the

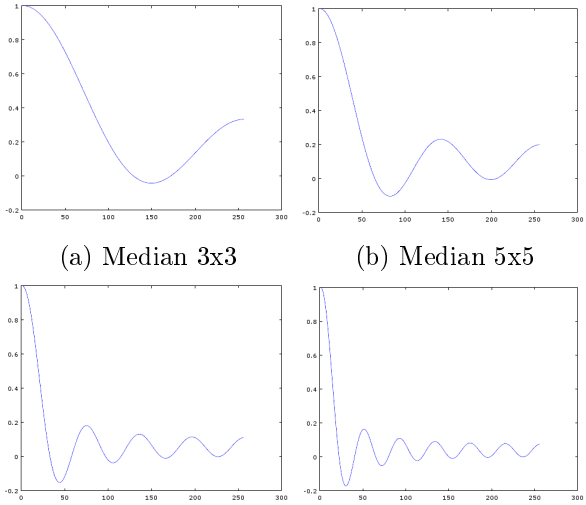

(a) Median 3x3 (b) Median 5x5

(c) Median 9x9 (d) Median 13x13

Figure 2: Graph of frequencies of an median operator in different dimensions

presence of subpixel shifts between low resolution observations. It should also be noted that the decimation operation adopted and described in most cases in the literature [3] follows a simplified model to represent the nature of the process. This simplified approach is done consistently by the use of a mean operator. Figure 2 shows the graph of frequency values considering operators of different dimensions. It is possible to note that the higher the matrix of the median operator, the more often the frequencies have zero values or even negative values, clearly showing that frequencies that may be important for the super-resolution process end up being discarded by the characterization of the model Adopted in the decimation process. The hybrid proposal addressed has the objective of precisely recovering the lost partial frequencies that can be valuable to obtain a good high resolution estimation.

3. Methodology

3.1 Subpixel displacement

In this work the values of the displacements are used for the generation of the PSF values and therefore, an approach is necessary to estimate the displacements at the subpixel level and that it proves useful for the necessity of the problem to be treated [11, 12]. The chosen iterative method [12](Irani-

Peleg) only considers the low resolution images degraded and with relative displacements between them following a global translation movement, not considering any other types, however, the approach supplies the necessities considering the sets of images that will be used for the experiments. Therefore, consider two continuous signals f, g: $\Re^2 \rightarrow \Re$ representing a reference image and a slightly offset version thereof, respectively. Thus, we need to find x_0 and y_0 that minimize a similarity function given by

$$s(x_0, y_0) = \sum_{x \in X} \sum_{y \in Y} [f(x, y) - g(x - x_0, y - y_0)]^2 \tag{2}$$

where X and Y are finite sets of points. Assuming that $f(x, y)$ and $g(x, y)$ are analytic functions, and by expanding $g(x, y)$ for the first term of its Taylor Series, it is easy to show that X_0^* and y_0^* that minimize the equation 2 is given by equations 3 and 4, respectively,

$$x_0^* = \frac{\sum_x \sum_y [(f - g)(x, y) - y_0^* g_y(x, y)] \, g_x(x, y)}{\sum_x \sum_y g^2 x(x, y)} \tag{3}$$

$$y_0^* = \frac{\sum_x \sum_y [(f - g)(x, y) - x_0^* g_x(x, y)] \, g_y(x, y)}{\sum_x \sum_y g^2 y(x, y)} \tag{4}$$

$g_x(x, y)$ e $g_y(x, y)$ represent the first derivative of $g(x, y)$ with respect to x and y, respectively.

Thus, it is possible to obtain the displacements in both directions, vertical and horizontal, to be used in the POCS algorithm proposed in this work.

3.2 Reference POCS Algorithm

The reference algorithm used comes from the work of Tekalp et al. [13]. Therefore, for the solution formulation, consider a J amount of low resolution frames with dimensions of MxM pixels, aiming to reconstruct based on them a high resolution image with dimensions of NxN pixels, considering that $M < N$, that is, the HR image obtained will have larger dimensions than the LR images considered. The low-resolution frames will be denoted by $d_j(m, n), m, n = 0, 1, ..., M - 1$ and $j = 1, 2, ..., J$. The image to be estimated and therefore still unknown, high resolution will be denoted by $f(k, l), k, l = 0, ..., N - 1$. We therefore have N^2 unknown values to be estimated (being N^2 gray scale values and N^2 locations) and JM^2 equations to be estimated. Disregarding initially the presence of noise, each frame of low resolution can be obtained in relation to a high resolution image from the equation 5,

$$d_j(m,n) = \sum_{k=0}^{N-1}\sum_{l=0}^{N-1} f(k,l)h_j(m,n;k,l) + v_j(m,n) \tag{5}$$

$j = 1, ..., J$. The j index in h_j and v_j refer to the frame number to be considered, thus establishing that the PSF and noise values may be different in each frame.

It is necessary to define that $h_j(m,n;k,l)$ is the point spread function (PSF) variant in space and $v_j(m,n)$ is the additive noise. From the equation 5, we can see that $JM^2 = N^2$, so it is possible to determine exactly the N^2 pixels with gray level of the image HR $f(k,l)$.

We can calculate an equivalent manner, the point spread function (PSF) $h_j(m,n;k,l)$ as follows:

$$h_j(m,n;k,l) = \frac{A_j(m,n;k,l)}{A_L} \tag{6}$$

where $A_j(m,n;k,l)$ is the area of overlap between the pixel LR with center in (m,n) and the pixel HR with center in (k,l) and A_L is the area of the LR pixel.

To detail the reconstruction process by POCS, we need to reconsider the equation 5 without additive noise, inserting modifications,

$$0 = d_j(m,n) - \sum_{k=0}^{N-1}\sum_{l=0}^{N-1} f(k,l)h_j(m,n;k,l) \tag{7}$$

where $d_j(m,n)$ are the known LR frames and we consider that $h_j(m,n;k,l)$ has also been calculated and has its known values. If we do not know $f(k,l)$ we can try to find it through the different versions of $y(k,l)$, which will be estimated in each iteration of the POCS regularizing process, considering the equation 8.

$$\varepsilon_j'(m,n;y) \triangleq d_j(m,n) - \sum_{k=0}^{N-1}\sum_{l=0}^{N-1} y(k,l)h_j(m,n;k,l) \tag{8}$$

A good choice for y is that in which the result of the above equation is the smallest possible, on the other hand, a bad choice would cause a larger error with respect to the desired image $f(k,l)$. The best choice will be that in which $y(k,l)$ can get $f(k,l)$ or get close to the maximum, which would make it as close to zero as possible. Considering the presence of the noise, ε_j' will be represented by:

$$\varepsilon'_j(m,n;y) \triangleq \varepsilon'_j(m,n;y) + v_j(m,n) \tag{9}$$

Considering the above, one approach to solve the problem is to force ε'_j to y to be restricted, that is, the values will have a limited magnitude. Considering this reasoning we can then represent this modeling through a convex set given by:

$$C_j(m,n) \triangleq y : |\varepsilon'_j(m,n;y)| \leq \eta \tag{10}$$

where η is a conveniently chosen constant, suggesting the use of $\eta = 3\sigma$ and σ is the standard deviation of noise $v(m,n)$.

From the definition of the main restriction set of the POCS approach on which we base our work, we can then define how to calculate the projectors that will be used to estimate the high resolution image.

For POCS projectors, three cases need to be considered:
(i) $\varepsilon'_j(m,n;y) > \eta$, (ii) $\varepsilon'_j(m,n;y) < -\eta$ e (iii) $-\eta \leq \varepsilon'_j(m,n;y) \leq \eta$. Therefore, the projector that will be used for the case (i), will be:

$$y^*(k,l) = q(k,l) + \frac{\varepsilon'_j(m,n;y) - \eta}{||h_j||_F{}^2} h_j(m,n;k,l) \tag{11}$$

For case (ii), the projector will be similarly:

$$y^*(k,l) = q(k,l) + \frac{\varepsilon'_j(m,n;y) + \eta}{||h_j||_F{}^2} h_j(m,n;k,l) \tag{12}$$

For case (iii) since the values are within the magnitude considered, no modifications are required in the value of the analyzed pixel, $y^*(k,l) = q(k,l)$. It is also important to clarify that $||h_j||_F{}^2$ is Frobenius Norm of PSF.

3.3 Hybrid approach and the modified Richardson-Lucy algorithm

Considering the proposed methodology, the objective is to improve the POCS approach through restoration techniques that can be modeled within a set of convex constraints. Considering that the implemented POCS algorithm already considers information derived from the LR images and the PSF that was modeled through the overlapping of the pixels, it is also necessary to condition the estimation in each interaction in such a way as to regularize the bad conditioning and recover frequencies that were lost by the process of decimation of the images used, preserving edges and details that are important to obtain good results. Thus, the proposed approach uses the Richardson-Lucy algorithm, however, modified by using it together with the Canny filter.

The Richardson-Lucy (RL) [14, 15] algorithm is a widely used technique for image restoration, usually for partial frequency recovery, and is derived from the maximum likelihood expression for images where additive noise has a Poisson or Gaussian distribution. The algorithm RL for the iterative solution of $f(x, y)$, for a Gaussian noise, is given by

$$\widehat{f}_{n+1}(x,y) = \left\{ \left[\frac{g(x,y)}{\widehat{f}(x,y) * h(x,y)} \right] * h(x,y) \right\} \cdot \widehat{f}_n(x,y) \tag{13}$$

where n is the index for iteration number and $g(x, y)$ is a blurred and noisy version of the observed image.

Considering the equation 14, $f(x, y)$ is the image to be obtained through the RL-CANNY approach, through the weighted filter p (normalized Canny filter) and the image generated by the Richardson-Lucy algorithm.

$$f(x,y) = f_n(x,y) * p + g(x,y) * (1-p) \tag{14}$$

This RL-CANNY approach will be considered as a convex constraint set to be added in the POCS formulation and therefore, its projector can be represented by the equation 15,

$$O_n = \left[\left(\frac{g}{\widehat{f}_{n-1} * h} \right) * h \right] \tag{15}$$

and its constraint set is formulated by 16.

$$C_{rl}^n = \left\{ \widehat{f}_n : O_n \cdot \widehat{f}_{n-1} \right\} \tag{16}$$

The demonstrations on the convexity of the set and the formulation of the projectors have been omitted but can be found in the reference [16].

4. Results

The work of Farsiu et al. developed by the research laboratory in signal processing of the University of California, Santa Cruz, to carry out comparative studies between the approach proposed in this work and the studies developed by the aforementioned research group.

For discussion of the results, we will use three different versions of the POCS approach. POCS1 is the original reference algorithm in its sequential form and POCS2 is the same modified algorithm for the parallel projection form. POCS3 has the sequential formulation with the addition of a further

convex restriction set containing the approach using the Richardson-Lucy algorithm modified by the weighted contribution of the Canny filter, which represents the hybrid approach.

POCS algorithms need an initial estimate of the high resolution image. In the obtained results, a low resolution image of the considered set was used, amplified through an order 0 interpolation (pixel replication) avoiding the blurring caused by other approaches that can influence in the high resolution image estimation process.

For the tests, 7 (seven) low resolution images of the EIA image set were considered. One of them was chosen to be considered the reference image in obtaining the displacement values between it and the other 6 remaining images through the Irani-Peleg motion estimation algorithm. These seven images were therefore considered as convex sets in the POCS algorithm.

We consider that the standard deviation of the noise of the images σ is equal to 1 and therefore the value of η is 3 ($3 * \sigma$), value obtained in heuristic form after several tests performed. For POCS1 and POCS3, 15 iterations were required and for POCS2, only 10 iterations were sufficient. A single standard deviation value of noise was defined for all images, taking into account that the way of obtaining the LR images are similar and therefore, the noise levels do not tend to have significant discrepancies between the images. It should be noted that the high resolution estimate to be obtained by the POCS algorithms is twice as large (180x180) than the low resolution images considered in the process (90x90).

Table 1: MSE values in relation to original resized EIA image

Results	*POCS1*	*POCS2*	*POCS3*
MSE	2713,3	2410,9	1754,8

By analyzing the results, it can be seen that POCS3 tends to preserve edges better and attenuate variations in pixel intensities in the gray and uniform regions of the image. Table 1 shows the values obtained by the MSE of the three POCS approaches to the original image resized to 180x180. The values show that POCS3 tends to be closer to the high resolution image compared to POCS1 and POCS2, which is also notable considering the visual analysis of the images. The MSE values demonstrate the evolution of the POCS1, POCS2 and POCS3 algorithms. The POCS3 algorithm has a significant reduction of the MSE compared to the other POCS approaches

considered.

The figure 4 shows the results to which Farsiu et al. Performed comparisons with the Robust Super-Resolution (L1 + Bilateral TV) algorithm in his published works, together with the estimate obtained by POCS3.

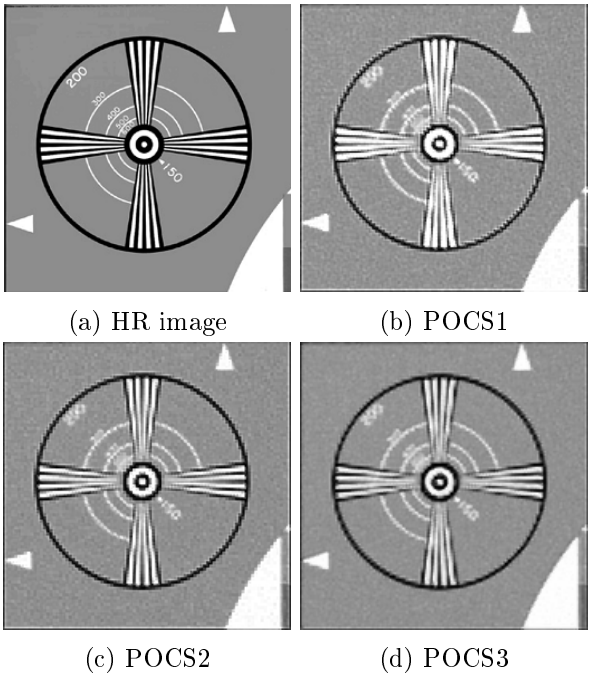

(a) HR image (b) POCS1

(c) POCS2 (d) POCS3

Figure 3: Comparison between the images: (a) Original HR, (b) Estimation Result obtained by POCS1 algorithm, (c) Estimation Result obtained by POCS2 algorithm and (d) Estimation Result obtained by POCS3 algorithm

Farsiu et al. [6, 5] used the following parameters to generate the result in letter (h) of Figure 4: $\lambda = 0.005$, Step Size $P = 2$, $\beta = 110$ e $\alpha = 0.6$, using 50 iterations to obtain the result, considering a magnification of 4 times the size of the low resolution images.

A possible justification for the result using the EIA image set by the proposed approach still distances itself from the result obtained by Farsiu et al. [6, 5] through Robust Super-Resolution, is precisely the difference of magnifying factors. Although it is a disadvantageous comparison, because the parameters for obtaining the results are described in the articles used for comparison, we consider that these are the best results obtained using the robust approach and, therefore, would allow a consistent analysis of the

results.

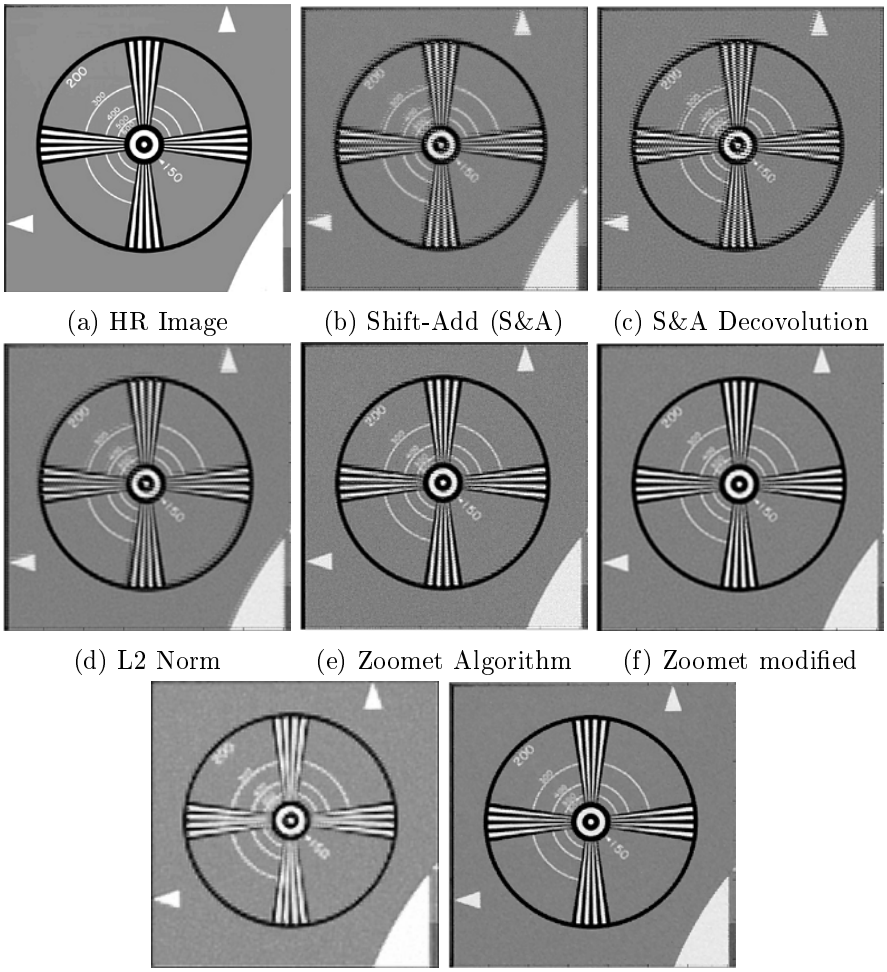

(a) HR Image (b) Shift-Add (S&A) (c) S&A Decovolution

(d) L2 Norm (e) Zoomet Algorithm (f) Zoomet modified

(g) POCS3 (h) L1 + BilateralTV

Figure 4: Comparison between the images:(a) Image HR, (b) Shift and Add (S&A), (c) Shift and Add (S&A) with Deconvolution, (d) L2 Norm, (e) Zoomet, (f) Zoomet with Regularization, (g) POCS3 e (h) L1 + BilateralTV (Robust Super-Resolution)

However, we performed some tests with the Robust Super-Resolution approach through software developed by the authors to generate the result of the EIA image considering a magnification factor of 2, as shown in Figure 5. The parameters considered were: $\lambda = 0.01$, Step Size $P = 2$, $\beta = 2$

and $\alpha = 0.6$, using 30 iterations to obtain the result. These values were obtained after several tests. The result obtained (L1 + BilateralTV) from the reported parameters shows a worsening of the estimation obtained by the robust framework. One justification would be that the information a priori in this case is smaller and undermine the performance of the algorithm. However, considering that the proposed hybrid approach obtained the estimate considering the same magnification, the POCS3 result in this case is higher.

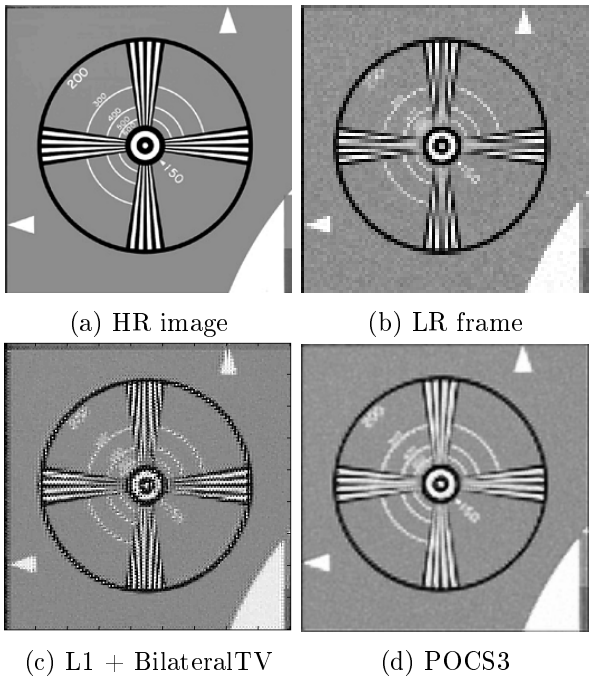

(a) HR image (b) LR frame

(c) L1 + BilateralTV (d) POCS3

Figure 5: Comparison of the images: (a) Original HRb) Low resolution image (c) Result obtained L1 + Bilateral TV (d) Estimation Result obtained by the algorithm POCS3

We also performed tests with the hybrid approach (POCS3) with the results of the Robust Super-Resolution (L1 + BilateralTV), considering the set of Surveillance (small) images [Figura 6]. For the generation of the results by the technique (l1 + Bilateral TV) the following values were used for the parameters: $\lambda = 0.01$, Step Size $P = 2$, $\beta = 2$ and $\alpha = 0.6$, using 30 iterations in obtaining the result.

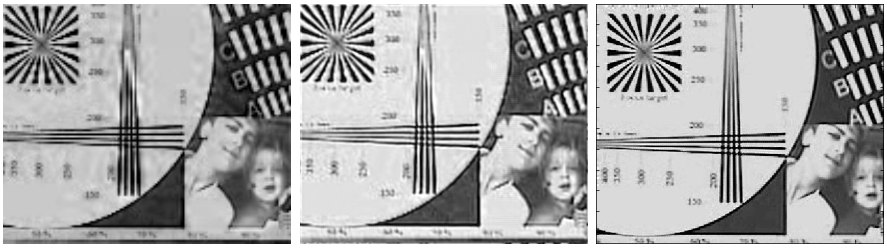

(a) LR frame (b) POCS3 (c) (L1+BilateralTV)

Figure 6: Comparison between the images: frame LR (a), proposed method (b) and Robust Super-Resolution (L1 + BilateralTV) algorithm (c)

For the generation of the high resolution estimate by POCS3 in this case, it was considered 20 iterations only, in which we did not notice significant changes considering a greater number of iterations. For both the POCS3 and the Robust Super-Resolution approach, the estimates generated are two times larger (230x236) than the low-resolution (115x118) Surveillance (small) images considered.

It is possible to note through the visual comparison of the images (b) POCS3 and (c) L1 + Bilateral TV (Robust Super-Resolution) in Figure 6 that the proposed algorithm presents a good result for the set of images Surveillance (Small) with performance close to that obtained by the L1 + Bilateral TV technique. Some numbers in the image can be viewed and detected, just as the existing borders had their pixelization reduced. We can also highlight that the background and other regions of the image have a smoother transition between the gray levels compared to the low resolution version (a).

4. Conclusion

Considering the presented results, there was a good performance of the POCS algorithms showing an interesting evolution in the comparison between the POCS1, POCS2 and POCS3 approaches. The proposed approach (POCS3) had good results when compared to the Robust Super-Resolution (L1 + Bilateral TV) algorithm, considering the same magnification factor. However, the comparison with results considering a larger magnification, in four times the size of the low resolution image, demonstrates that the performance of the proposed algorithm was inferior to the algorithm of Robust Super-Resolution (L1 + Bilateral TV) for the case of the set of Images, which has a greater degradation. We emphasize that we need to take into account the significant difference between magnification factors, because the hybrid ap-

proach only increases the size of the low resolution image in two times in all cases compared. Surveillance (small) images, although not as degraded as EIA images, have important aspects to be recovered in the high resolution estimation, in which the hybrid algorithm (POCS3) showed to be very close to the algorithm at which was compared, considering that the results obtained by both techniques have the same dimensions.

We believe that the hybrid methodology (POCS3) has the potential to approach or even overcome the Farsiu et al. [6, 5]. The results show that algorithms based on Projections on Convex Sets (POCS) can generate appreciable results through a few iterations and have an important flexibility that allows to aggregate other methods that can be formulated as convex sets that can add and improve the obtained results even more, generating appreciable results that approximate or surpass newer techniques of the literature.

References

[1] R. C. Gonzalez and R. E. Woods, *Digital Image Processing (3rd Edition)*. Upper Saddle River, NJ, USA: Prentice-Hall, Inc., 2006.

[2] S. Chaudhuri, *Super-Resolution Imaging*. Norwell, MA, USA: Kluwer Academic Publishers, 2001.

[3] S. C. Park, M. K. Park, and M. G. Kang, "Super-resolution image reconstruction: a technical overview," *IEEE signal processing magazine*, vol. 20, no. 3, pp. 21–36, 2003.

[4] P. Milanfar, *Super-resolution imaging*. CRC Press, 2010.

[5] S. Farsiu, D. Robinson, M. Elad, and P. Milanfar, "Advances and challenges in super-resolution," *International Journal of Imaging Systems and Technology*, vol. 14, no. 2, pp. 47–57, 2004.

[6] S. Farsiu, D. Robinson, M. Dirk, M. Elad, and P. Milanfar, "Fast and robust multiframe super resolution," *IEEE Transactions on Image processing*, vol. 13, no. 10, pp. 1327–1344, 2004.

[7] S. C. Park, M. K. Park, and M. G. Kang, "Super-resolution image reconstruction: a technical overview," *IEEE Signal Processing Magazine*, vol. 20, no. 3, pp. 21–36, 2003.

[8] S. Borman and R. Stevenson, "Spatial resolution enhancement of low-resolution image sequences-a comprehensive review with directions for

future research," *Lab. Image and Signal Analysis, University of Notre Dame, Tech. Rep*, 1998.

[9] M. R. P. Homem, "Reconstrução tridimensional de imagens com o uso de deconvolução a partir de seções bidimensionais obtidas em microscopia óptica," *Doutorado em Física Computacional, Universidade de São Paulo-Instituto de Física de São Carlos*, 2003.

[10] R. S. Babu and K. E. S. Murthy, "A survey on the methods of super-resolution image reconstruction," *International Journal of Computer Applications*, vol. 15, pp. 1–6, February 2011.

[11] D. Keren, S. Peleg, and R. Brada, "Image sequence enhancement using sub-pixel displacements," in *Computer Vision and Pattern Recognition, 1988. Proceedings CVPR'88., Computer Society Conference on*, pp. 742–746, IEEE, 1988.

[12] M. Irani and S. Peleg, "Improving resolution by image registration," *CVGIP: Graphical models and image processing*, vol. 53, no. 3, pp. 231–239, 1991.

[13] A. M. Tekalp, M. K. Ozkan, and M. I. Sezan, "High-resolution image reconstruction from lower-resolution image sequences and space-varying image restoration," in *Acoustics, Speech, and Signal Processing, 1992. ICASSP-92., 1992 IEEE International Conference on*, vol. 3, pp. 169–172, IEEE, 1992.

[14] W. H. Richardson, "Bayesian-based iterative method of image restoration," *JOSA*, vol. 62, no. 1, pp. 55–59, 1972.

[15] L. B. Lucy, "An iterative technique for the rectification of observed distributions," *The astronomical journal*, vol. 79, p. 745, 1974.

[16] H. Stark, Y. Yang, and Y. Yang, *Vector space projections: a numerical approach to signal and image processing, neural nets, and optics*. John Wiley & Sons, Inc., 1998.